

A Thesis Presented to
The Faculty of Alfred University
Conditions of Powder Flow and Fill

By
Samantha J. Kotze
&
Ryan M. Fowler

In partial fulfillment of
the requirements for
the Alfred University Honors Program

May 2020

Under the Supervision of:
Chair: Dr. William Carty, Chair of Ceramic Engineering
and Glass Engineering Sciences
Committee Members:
Dr. Gabrielle Gaustad, Dean of Inamori School of Engineering
Hyojin Lee, Professor of Ceramic Engineering

Acknowledgments

We would like to thank the individuals whose support enabled us to complete this thesis. Special thanks to Dr. William Carty for being our advisor and guiding us through this process. To Andy Wereszczak for helpful advice on this project. To Hyojin Lee for kindly imaging our samples when we were unable to. To Lucas Laing who was crucial in helping us build our testing apparatus. Finally, we want to give a huge thank you to our friends and family who have helped support us throughout our personal and academic career.

Table of Contents

Acknowledgments.....	ii
List of Figures	iv
List of Tables	v
Honors Foreword	vi
Abstract	xi
1. Introduction.....	1
2. Literature Review.....	2
2.1 Particle Systems	2
2.2 Angle of Repose	2
2.3 Powder Flow Measurement.....	3
2.4 Uniform Die Fill.....	5
2.5 Agglomeration.....	6
3. Experimental Approach	8
3.1 Powder Flow	8
3.2 SEM Imaging	12
4. Results and Discussion	13
4.1 Calculations.....	13
4.2 Powder Flow	15
4.3 Images of particles	22
5. Conclusion	28
7. References.....	30

List of Figures

Figure 1. Measurement of AOR. ⁵	3
Figure 2. Image of apparatus built for powder flow testing.	9
Figure 3. Schematic of apparatus built for powder flow testing	9
Figure 4. Image that illustrates surface roughness inflicted from sanding process.	10
Figure 5. Plot of flow angle vs particle mass.....	14
Figure 6. Plot of density of particles and their critical flow angles	17
Figure 7. Plot of first flow and critical flow angles	18
Figure 8. Plot of critical to first flow ratio and particle density.....	19
Figure 9. Plot of Critical Flow angle and log (Particle Mass).	20
Figure 10. Plot of angular velocity versus particle mass.	21
Figure 11. SEM images of glass sphere standard 1017a (Glass Spheres (III)).....	22
Figure 12. SEM images of glass sphere standard 1018a (Glass Spheres (II))......	22
Figure 13. SEM images of glass sphere standard NBS 1003 (Glass Beads (I)).	22
Figure 14. SEM image of critical flow for Strontium Carbonate.	23
Figure 15. SEM image of critical flow for China clay (Kaolin)......	23
Figure 16. SEM image of critical flow for calcined alumina (I).	23
Figure 17. SEM image of critical flow for Borax.	24
Figure 18. SEM image of critical flow for Silicon Carbide.....	24
Figure 19. SEM image of critical flow for calcined alumina (II).	24
Figure 20. SEM images of china clay critical flow samples.....	25
Figure 21. SEM images of china clay first flow samples.	25
Figure 22. SEM images of quartz (II) critical flow samples.....	26
Figure 23. SEM images of quartz (II) first flow samples.	26

List of Tables

Table I.	List of Powders used in this experiment.	11
Table II.	Powders imaged and their approximate particle mass.	13
Table III.	List of materials used and the recorded critical and first flow angles.	16

Honors Foreword

The path to my thesis topic was not a straightforward one, that is to say my topic changed and fluctuated often. The path to my thesis began over the summer, when I interned for the Dean of Engineering. I was completing preliminary research for a potential project on the ability to recycle tungsten carbide bits. This topic occupied the majority of my summer as we tried to brainstorm an effective, environmentally friendly method for recycling. With the help of Dr. Carty, my advisor, we settled on using a glass to break down the bit's structure, potentially creating the ability to reuse the material and the glass. After the summer was over, I was in search of a thesis topic and this project seemed like a perfect fit. Further it was an interesting topic, combining the metallurgical elements that I was less familiar with, with the thermodynamics basics I had learned about in my classes. The downside was I had no supplies and would have to wait to receive them before my work could begin.

Upon discussions with my advisor second semester he asked me to switch my thesis entirely. I had recently accepted a job offer with Any Wereszczak at Oak Ridge National Lab. Dr. Carty had a project in mind that would fit nicely into the work I will be completing for Andy in my upcoming position. It not only prepares me for the subject matter of my future work, but it also gives me an introduction to the lab atmosphere I will be working in. Consequently, I switched my entire project with only one semester to go. I had to be flexible and adjust once again.

Initially, this project had a rough beginning due to the late start and lack of materials. I was paired with a partner and we had a lot of potential testing to cover. Our

general direction was particle packing; we needed to try to determine a simple method to analyze flow behavior accurately. Flow behavior refers to the interaction of the particles with each other and any contact surface. Ideally, we want materials and specifically powders that will easily move or flow, this allows for efficient packing. Well flowing materials, often referred to as free-flowing materials, can pack more efficiently because the particles can easily rearrange without sticking to the other particles in the material. This is crucial because in ceramics one of the largest concerns is uniform packing and density. If the material does not pack uniformly, it will not have a uniform density. This is problematic because this will create defects in the final product. As with many things, problems compound themselves throughout the process. So, what started as an agglomerated powder turned into a low-density product that will not meet production standards.

Although the solution to the problem may seem obvious, it is far more complex. The complexity is partially due to the sheer number of materials and processes in the ceramic industry. This is further complicated by the lack of universal measuring ability and the large number of factors that affect particle flow and packing. In general, there is still a large amount of research to be done in the areas of particle flow and packing, in order to better understand what occurs and how to process materials.

As a whole, the ceramic industry is trying to move to a global approach. Currently, most testing and processing is based on particular equipment and production processes, this is inefficient because if the equipment or raw materials change, the process cannot be easily adjusted. Further it is difficult to compare testing and results between studies, plants, and processes when there is such large variability in testing

procedure. As a result, there is a push to work globally and define processing parameters that can be used over a broad range of processes and materials. Our thesis incorporates this idea, as we hypothesize that there is a critical particle mass or minimum particle mass necessary for free flow. In theory this cutoff could be applied to a broad range of materials, therefore creating a simple but effective method for characterizing flow behavior. This would also allow for more informed processing and design of processing equipment.

Our testing began with the thought to place a small amount of material on a surface and then rotate this surface, measuring the angle where the powder flowed. This turned out to be more difficult than originally expected. Our advisor recommended that we use a copper plate as the contact surface. Copper is a good choice as we wish to eliminate a build-up of charges on the plate. The lack of charge build-up will limit the particle-surface interactions and allow for a more accurate measurement of flow behavior. The plate was also lightly sanded to reduce particle sliding. The idea is that we want to be able to get true free flow, where the particles are tumbling down the plate not sliding off the plate because the surface is smooth. My partner, Ryan, and I started by going into the lab and experimenting with the copper plate. We found that it was quite difficult to reproduce each run, therefore we decided to build a simple stand to increase the reproducibility. This was a very simple apparatus made out of wood, which included blocks on the side to prop up the plate. This plate could be held against the stoppers, inclined, and then the angle where the powder began to move could be marked on the side of the stand. After which, an angle of flow could be calculated using trigonometry. These measurements were intended to be supplemented with SEM (scanning electron

microscope) images of the particles that flowed. SEM images of these samples will provide a visual observation of particle morphology and size, in addition to an estimated particle size.

We began to test the powders using this stand, but we were still trying to figure out the best way to proceed testing. We tested all the materials one time and had collected samples for further testing and imaging. This was a few days before spring break, so we packed up thinking we would be back in a week's time to finish collecting data. Of course, this is not what happened thanks to the pandemic.

I was visiting my sister for spring break when her school announced it was moving all classes online. This was incredibly confusing as this announcement seemed to come out of nowhere. Up to this point there was no reason to have expected the pandemic to affect my everyday life. Sure, hand sanitizer and disinfecting wipes were near impossible to find, but it was mostly life as usual. Suddenly, I was overwhelmed with emotions and rapidly changing circumstances. I waited in anticipation for Alfred to decide how we would proceed, anxious about all the unknowns.

Alfred decided to move classes online late one night and the next morning my Mom and I left to drive back to Alfred. I live in on-campus housing so there was quite the rush to try to avoid the craziness, to pack up, and to go home. It was truly something I would never forget. I ran into the labs, wildly trying to grab all my stuff and get out as soon as possible. Everything happened so quickly, I did not even process that I was probably leaving Alfred for the last time. There was so much uncertainty about how we would proceed, and I was naturally concerned about my research-based thesis.

Shortly after my return home, I talked to my advisor and he had wanted Ryan and I to return to Alfred to finish the remaining data. Unfortunately, this was unable to happen as both Ryan and I live on campus and both Pennsylvania and New York were quickly ushered into lock down. We then had to grapple with the concept of trying to complete a literary thesis on a topic where there was not a lot of literature available. Additionally, we had less resources at our disposal; we no longer had easy access to the library and lab. We combated this complication by trying to collect as much data as we could. I learned that even in a crisis research can continue, and data can still be collected. It was not easy, and we certainly could not have done it on our own. I had to create my own testing spaces in my house and find material I needed to test in depleted grocery stores and pet stores. We paired this with materials sent to us by our advisor and in lab research completed by Hyojin Lee. He was kind enough to sort through our samples and image them when we were unable to do so. Ultimately, this allowed us to gather enough data to be able to write a comprehensive thesis.

This crisis taught me to trust myself more and ask others for help when I need it. Despite everything, I could still work towards understanding not only my topic better but its implications on the larger ceramic field. This process confirmed to me that I want to do research in the ceramic field. While I am still unsure what area of ceramics I want to work in, this is an important topic in my field and will help me regardless of what area I choose. The Oak Ridge Lab is the first step in my post grad life and will allow me the space and opportunity to grow as a researcher and find my place in the ceramic engineering world.

Abstract

Understanding the conditions that contribute to powder flow are essential to anticipate the segregation of particles in flow situations. Although various methods are used to quantify powder flow and powder fill in industry, these methods fail to properly capture observed behavior, particularly as the particle size decreases, thereby failing to accurately predict powder flow, fill, and packing outside of a specific process. It is unclear if there is a specific boundary below which particle flow will not occur. The hypothesis of this study is that there is a correlation between particle size, density and flow behavior, and there is a critical particle mass necessary for free flow. This study analyzes the flow behavior of a broad range materials, including glass sphere standards 1018a, 1017a, and NBS 1003. The flow of these powders was analyzed by inclining a roughened copper plate until particles began to tumble. The copper plate dissipated electrostatic charge. The angles of both the onset of flow, when the first observation of movement occurred, and critical flow, where all the powder flowed, were recorded. Although two flow angles were identified for some of the powders, this does not necessarily mean there are two different flow behaviors. Rather this study purposes that the first flow is agglomerate or large particle flow and critical flow is either true powder flow or the gravitational forces overcoming the interparticle forces. The samples were imaged by SEM to estimate particle size for initial and critical flow. It can be concluded that the powder flow data is not affected by density and is mass independent.

1. Introduction

Anticipating and preventing the segregation of particles in flow situations requires an understanding of the conditions that contribute to powder flow. Various methods exist to analyze the flow behavior of powders, although these tests are typically best suited for specific processes. Further, these tests fail to explain the observed flow behavior as the particle size decreases. The hypothesis of this study is that there is a correlation between particle size, density and flow behavior, and there is a critical particle mass necessary for free flow.

In this experiment, a broad range of materials, including glass sphere standards 1018a, 1017a, and NBS 1003, were analyzed using an inclined plate of roughened copper. The location where the powder began to flow, where the particles began to tumble, was marked and the angle of flow was calculated using trigonometry. Two different angles were identified: first flow or the onset of flow and critical flow or bulk powder flow. This study purposes that these two angles are not two different flow behaviors. Instead the first flow is agglomerate or large particle flow and critical flow is either true powder flow or the gravitational forces overcoming the interparticle forces. Electrostatic charge was dissipated by the copper plate.

Images of these samples were then captured using a scanning electron microscope to analyze particle morphology and estimate a particle size. The data demonstrated that the hypothesis was incorrect.

2. Literature Review

2.1 Particle Systems

The behavior of a particle and subsequently the material as a whole is highly dependent on the forces acting on the particles themselves. A particle system that is considered to be granular or free flowing is desired for optimal fill and flow, as they allow for efficient particle arrangement.¹ This type of particle system occurs when the gravitational force is the dominant force acting on the particles, typically larger than 44 microns (opening in a 325-mesh sieve) for dry particles.² If the surface force is equal to the gravitational force, the material is said to naturally agglomerate.¹ In contrast, the material is considered colloidal when the surface forces are greater than the gravitational forces, which generally occurs for particles smaller than 20 micron.³

2.2 Angle of Repose

The angle of repose is one of the simplest ways to measure powder flow as this is demonstrated by simply pouring the material out onto a flat surface. The angle of repose (AOR) is the angle a material naturally forms when poured onto a horizontal surface, Figure 1 illustrates this angle.^{1, 4}

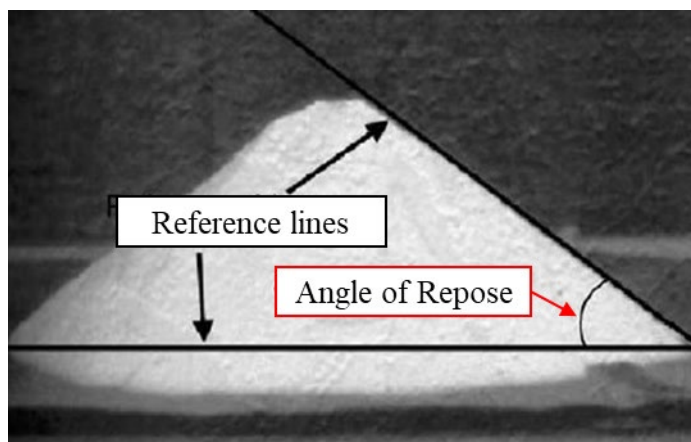


Figure 1. Measurement of AOR.⁵

In a larger, typically well flowing powder the angle of repose is smaller because the forces of gravity are dominant, pulling the particles closer to the surface thereby decreasing the AOR.¹ The AOR is proposed to be related to several factors including sliding and rolling friction, density of the particles, particle size, and shape.⁶ An increase in the sliding and rolling friction coefficients and increasing irregularity in shape, increases the AOR. In contrast, the AOR decreases with increasing particle size and container thickness.^{7,6} The AOR only slightly increases as the density of the particle increases, therefore the AOR is not sensitive to density.⁶ It is commonly agreed that the AOR relates to particle flow, however there are a variety of different methods to measure it, each resulting in slightly varying results. Ultimately, this means that the results are not necessarily comparable between methods.⁸

2.3 Powder Flow Measurement

As stated previously, there are a variety of tests that can be used to measure the angle of repose, resulting in discrepancies regarding ranges for flowability and AOR values. “Carr (1965 & 1970) and Raymus (1985) suggested that angles of repose below 30° indicate good flowability, 30°-45° some cohesiveness, 45°-55° true cohesiveness,

and >55° sluggish or very high cohesiveness and very limited flowability. Geldart et al. (1990) and Antequera et al. (1994) were more inclined to use the 40° criteria, based on the data of Brown and Richards (1970), in classifying free-flowing and cohesive powders.⁸ Further there is a lack of standardization regarding testing methods, such as amount of material, type, and size of equipment. In turn, this introduces further variance in the data.

One of these methods is Carr's compressibility index shown in Equation 1.

$$Carr = 100 * \left[1 - \left(\frac{bulk \ \rho}{tap \ \rho} \right) \right] \quad (1)$$

Tap density (tap ρ) refers to the density of the material after it has been tapped for a defined period of time and bulk ρ is the bulk density. The Carr index assumes if powders are easily compressed during tapping, the energy requirements for flow increases, preventing free flow.⁹ For a free-flowing powder, the Carr index is small, less than 10, because the bulk density and tapped density are similar. On the other hand, in a poor-flowing powder where there are greater interparticle interactions, the difference between the bulk and tapped density observed would be greater, and the Carr index would be larger, between 26-31.⁹

The Hausner ratio (HR) is calculated using Equation 2.

$$HR = \left(\frac{tap \ \rho}{bulk \ \rho} \right) \quad (2)$$

Where tap ρ is the tap density and bulk ρ is the bulk density. A large HR represents a larger difference between the tap and bulk density, if the HR is larger than 1.4, it is likely the material displays “all the properties of a cohesive powder.”⁵ Some studies have concluded that there is a good correlation between HR and AOR. The HR decreases as

the particle size increases, this is the same trend that is observed between AOR and particle size. Therefore, this suggests that an increase in particle size always decreases the cohesiveness of a powder.^{5, 8}

2.4 Uniform Die Fill

Uniform die fill refers to the filling of a die or cavity for pressing operations. In a pressing operation powder is pushed into the die and then the material is compacted. Uniform compaction behavior in dry pressing requires uniform die fill.¹⁰ Loose powders typically deposit at roughly 30% of their theoretical density, which is not sufficient to achieve a fully dense ceramic part.¹⁰ Flow is critically important to uniform die fill. Factors that affect die fill include cohesion and internal friction angle of the material, coefficient of friction between the powder and hopper, and size of the particles.¹¹ Powder cohesion is related to the intensity of interparticle forces including van der Waals, capillary, and electrostatic forces.³ The flowability of the material depends on the particle size distribution. Based on the Jenike classification, where the material is characterized using ff_c ratio of consolidation stress (σ_1) to unconfined yield strength (σ_c). Larger ff_c values indicate better flowing materials.¹² Materials below 20 μm are typically cohesive (ff_c 1-2), 20-38 μm samples are easy flowing (ff_c 4-10), 38-88 μm samples are on the border between easy and free flowing, and samples larger than 88 μm are free flowing (ff_c 10⁺).³

Additionally, size segregation should be avoided; it is the most influential factor affecting bulk uniformity.¹³ This causes there to be a concentration of large particles in some areas and a concentration of smaller particles in other areas, likely filling in the

void space created by the larger particles. Many factors contribute to size segregation including particle size, density, shape, cohesivity, and AOR. Turbulent, rather than smooth powder delivery can also cause size segregation. The most important of all of these is particle size. When particles are different sizes, they are subject to varied forces as they move, causing separation. Differences in particle diameter greater than a ratio of 1.3 to 1.0 allow particle segregation to occur. There is also evidence to suggest that the smaller, less than 30 microns, and more cohesive the material is, the less likely it is to separate.¹³ Ideally size segregation should be avoided to ensure the most uniform die fill, and consequently a dense and functional product.¹¹ This can be accomplished by limiting the number of processing steps after mixing, decreasing the difference in particle sizes, decreasing all particles to under 30 microns.¹³

2.5 Agglomeration

An important consideration in ceramic processing is the formation of agglomerates. Many ceramic powders form agglomerates, in part due to their small particle size. An agglomerate is defined as “a group of particles that are weakly bonded together, may behave as a fragile, larger pseudoparticle.”² In general, there are two different types of agglomerates, soft and hard agglomerates. Hard agglomerates are not easily broken as the particles are bonded together by primary chemical bonds, often formed during sintering or heating. The other type of agglomerate is a soft agglomerate, where particles are weakly bonded through “electrostatic, magnetic, van der Waals, or capillary adhesion” bonds rather than a chemical bond.² The presence of agglomerates in a given sample is believed to drastically alter the packing efficiency and flowability of

the sample, particularly in dry pressing operations. This is due to the large size difference between the un-agglomerated and agglomerated powder, preventing efficient particle rearrangement, and therefore preventing uniform packing and density.

3. Experimental Approach

3.1 Powder Flow

The experiment began with an idea for a test in mind: place powders of various chemistries, size distributions, and morphologies on a surface that could be put under an incline and measure the angle at which the powder flows. This data could then be cross referenced against data for density, particle size, and morphology to see if those characteristics produce a trend in angle of flow.

The apparatus used in this experiment was made from wood, whiteboard, and held together with screws. It was designed to have a plate be lifted to an angle, then when the operator observed the powder flow, the operator stopped tilting and immediately marked the edge of the plate with a pen. This allows for the measurement of an angle to be done quicker and more accurately than with a protractor. Figure 2 shows an image of the completed apparatus, which was used for the testing. Figure 3 shows a schematic of the apparatus, along with relevant labels and a marking for length l , which is used in Equation 1 to help calculate powder flow angles. Figure 3 also shows length W , the width of the copper plate and the angle of interest, θ , that is being calculated.



Figure 2. Image of apparatus built for powder flow testing.

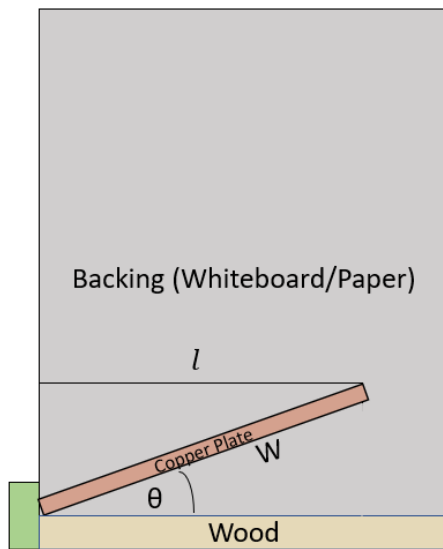


Figure 3. Schematic of apparatus built for powder flow testing.

The surface used for the inclination was a sanded copper plate. Copper was the desired surface because it does not maintain a static charge between the particles and the surface. The sanding roughened the surface to minimize the potential for particle sliding. Particle sliding is undesirable as it does not represent flow. Sanding was done by hand with a 120-grit sandpaper first for one minute and then 220-grit sandpaper for one minute

immediately following. Close attention was paid to the plate during sanding to ensure uniform abrasion of the copper surface. Figure 4 shows the surface roughness inflicted from sanding the plate.

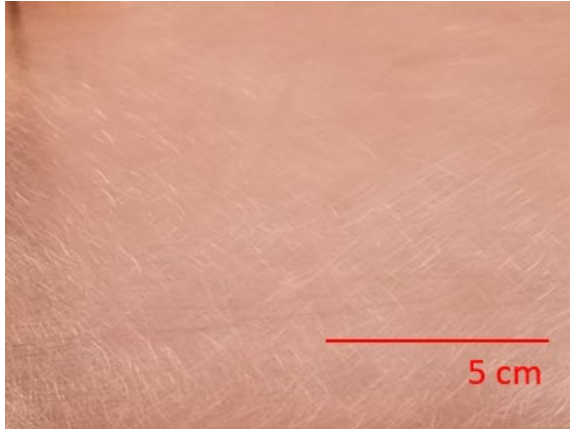


Figure 4. Image that illustrates surface roughness inflicted from sanding process.

29 powders were used to evaluate powder flow. Powders were simply selected from the powders available in the lab. Table I lists the powders with density and the measured flow angles, along with their more common commercial names, if applicable.

Table I. List of Powders used in this experiment.

Number	Material	Commercial Name	Density (g/cm ³)
1	Glass Beads (I)	1003 NBS Standard ¹⁴	2.54
2	Glass Spheres (II)	1018a NBS Standard ¹⁴	2.54
3	Glass Spheres (III)	1017a NBS Standard ¹⁴	2.54
4	Magnesium Carbonate		2.96
5	Zinc Oxide		5.10
6	Lithium Carbonate		2.11
7	Talc		2.71
8	Feldspar (I)	Minspar 200	2.56
9	Tabular Alumina	T-64 325 mesh	3.95
10	Calcined Alumina (I)	A-16 S.G. (Almatis)	3.95
11	Calcined Alumina (II)	A-10 (Almatis)	3.95
12	Mullite	Mulcoa 63	3.12
13	MgCa Borate	Hydroborasite ¹⁵	2.21
14	Calcium Hydroxide		2.21
15	Strontium Carbonate		3.74
16	Yttrium Oxide		5.01
17	Silicon Carbide	Crystal SiC 200 Grit	3.21
18	Barium Carbonate		4.29
19	Calcium Carbonate		2.71
20	Glass frit	Frit 3110	2.49
21	Magnesium Aluminate	Spinel	3.58
22	Quartz (I)	Min-U-Sil	2.65
23	Nepheline Syenite	A400	2.59
24	Bentonite		2.50
25	Borax		1.73
26	Feldspar (II)	G-200	1.09
27	Quartz (II)	Sil-Co-Sil	2.65
28	China Clay (Kaolin)	Grolleg	2.60
29	Ball Clay	Old Mine #4	2.60

The copper plate was placed in the corner of the wood, shown in Figures 2 & 3, and this was repeated before every test to ensure accuracy and repeatability. A piece of paper was placed on the whiteboard backing, perpendicular to the orientation of the copper plate as seen in Figure 2 to allow ease of recording the location of the onset of

flow. Next, a small amount of powder was poured somewhere on the plate in a shallow layer. The location of the powder did not matter experimentally since the whole plate is always subject to the same angle. Once the powder was placed on the plate, the plate was inclined until there was movement in the powder. A preliminary shuffle, denoted as “first flow,” was observed for all but three powders before the powder underwent a “critical flow” where all powder flowed off the plate. Once the locations for the first and critical flows of the powders were marked on the paper, the operator measured from the edge of the paper to the marks and wrote the length, denoted as l . The angle of the plate was calculated using Equation 3, when l is the distance on the backing material from the far left side to the inclined point of the copper plate and W is the width of the plate, which is always 20.32 cm (8 inches). This can also be visualized from Figure 3.

$$Angle = \arccos \frac{l}{W} \quad (3)$$

3.2 SEM Imaging

Samples were imaged using a scanning electron microscope with a spot size of 3.0 and an accelerating voltage of 20 kilovolts. Magnification was different for each powder imaged, depending on the size of the particles in that powder. These SEM images and ImageJ software (National Institutes of Health, 1.51j8) were used to estimate an average particle diameter for each sample.

4. Results and Discussion

4.1 Calculations

The average particle size for each imaged powder was used to calculate the particle mass assuming a spherical particle morphology and incorporating the skeletal density (ρ_{particle}) values using Equation 4. The density values were not corrected for agglomeration. Particle volume was calculated with the assumption that particles are spherical.

$$Mass_{\text{particle}} = Volume_{\text{particle}} * \rho_{\text{particle}} \quad (4)$$

The calculated particle mass for each of the imaged particles is tabulated in Table II. The calculated particle mass illustrated in Table II is plotted with critical and first flow angle in Figure 5.

Table II. Powders imaged and their approximate particle mass.

Material Number	Material	Critical Flow Size (μm)	Density (g/cm^3)	Particle Mass (g)
1	Glass Beads (I)	20.9	2.54	6.08E-09
2	Glass Spheres (II)	569	2.54	1.23E-04
3	Glass Spheres (III)	206	2.54	5.84E-06
10	Calcined Alumina (I)	0.43	3.95	6.62E-14
11	Calcined Alumina (II)	107	3.95	6.33E-07
12	Mullite	3.99	3.12	4.14E-11
14	Calcium Hydroxide	1.92	2.21	3.27E-12
15	Strontium Carbonate	24.4	3.74	1.13E-08
16	Yttrium Oxide	4.84	5.01	1.19E-10
17	Silicon Carbide	182	3.21	4.11E-06
21	Magnesium Aluminate	3.60	3.58	3.51E-11
25	Borax	148	1.73	7.40E-07
26	Feldspar (II)	4.48	1.09	2.06E-11
27	Quartz (II)	1.70	2.65	2.72E-12
28	China Clay (Kaolin)	5.58	2.60	9.44E-11

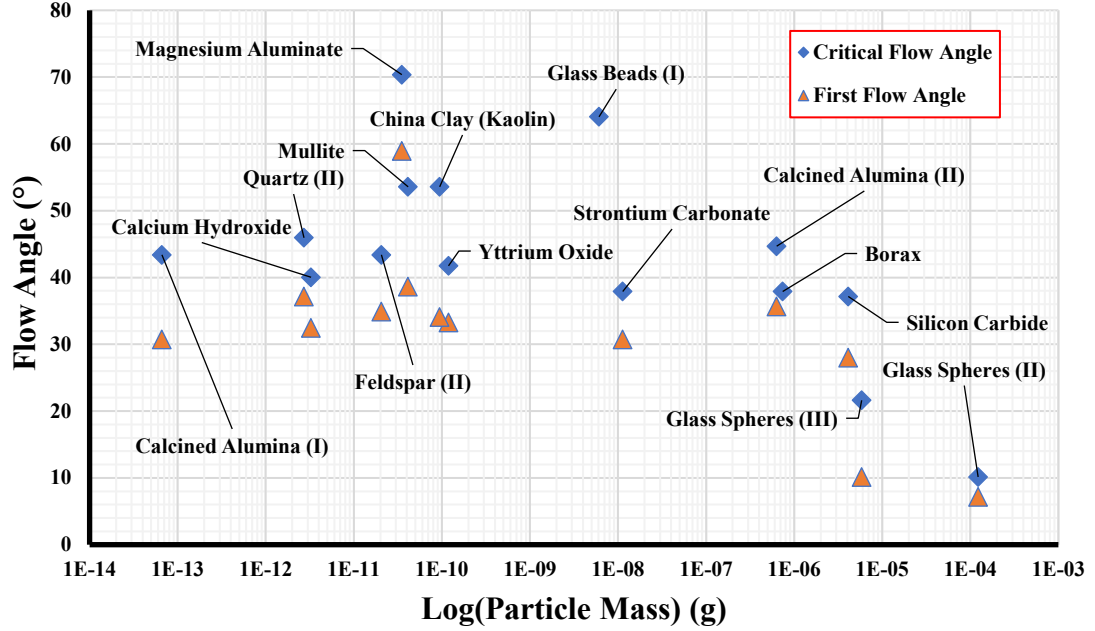


Figure 5. Plot of flow angle vs particle mass.

As a way to normalize the data, the inclined angle and the particle size results were used to calculate an angular velocity. To calculate the angular velocity, the linear velocity is calculated first (Equation 5) and that value is used to calculate the angular velocity (Equation 6).

$$V_{linear} = 2 * (9.8 * \sin(\theta_{critical})) * d \quad (5)$$

Equation 5 was used where 9.8 was used as the acceleration vertically due to gravity in meters per second squared. $\theta_{critical}$ was used to denote the critical flow angle found in Table III. The variable d was used as a distance that the powder tumbled down the plate, assumed to be 7.62 cm (3 inches) for all powders. This equation has some assumptions that come with it. Particles are first assumed to be spherical, as is the assumption in this whole study. Also, particles are assumed to be rolling and not sliding,

which was further supported after sanding the surface of the copper plate. Equation 6 connects the calculated value for linear velocity from equation 5 and incorporates radius to calculate the angular velocity which has units of ((m/s)/m), or, 1/s.

$$V_{angular} = \frac{v_{linear}}{radius_{particle}} \quad (6)$$

4.2 Powder Flow

Table III lists the materials used and the critical and first flow angles. Figure 6 shows the relationship between the density of the powders and critical flow angle.

Table III. List of materials used and the recorded critical and first flow angles.

Material Number	Material	Density (g/cm ³)	Critical Flow Angle (°) (θ_{critical})	First Flow Angle (°) (θ_{first})
1	Glass Beads (I)	2.54	64.06	N/A
2	Glass Spheres (II)	2.54	10.14	7.17
3	Glass Spheres (III)	2.54	21.61	10.14
4	Magnesium Carbonate	2.96	42.75	29.87
5	Zinc Oxide	5.10	38.62	34.09
6	Lithium Carbonate	2.11	54.68	34.88
7	Talc	2.71	60.00	34.09
8	Feldspar (I)	2.56	47.18	38.62
9	Tabular Alumina	3.95	47.18	33.29
10	Calcined Alumina (I)	3.95	43.40	30.75
11	Calcined Alumina (II)	3.95	44.69	35.66
12	Mullite	3.12	53.58	38.62
13	MgCa Borate		42.75	33.29
14	Calcium Hydroxide	2.21	40.04	32.46
15	Strontium Carbonate	3.74	37.90	30.75
16	Yttrium Oxide	5.01	41.75	33.29
17	Silicon Carbide	3.21	37.17	28.02
18	Barium Carbonate	4.29	41.41	37.17
19	Calcium Carbonate	2.71	43.40	35.66
20	Glass Frit		40.04	35.66
21	Magnesium Aluminate	3.58	70.37	58.96
22	Quartz (I)	2.65	42.08	N/A
23	Nepheline Syenite	2.59	42.75	38.62
24	Bentonite	2.50	49.58	38.62
25	Borax	1.73	37.90	N/A
26	Feldspar (II)	1.09	43.40	34.88
27	Quartz (II)	2.65	45.95	37.17
28	China Clay (Kaolin)	2.60	53.58	34.09
29	Ball Clay	2.60	45.95	36.42

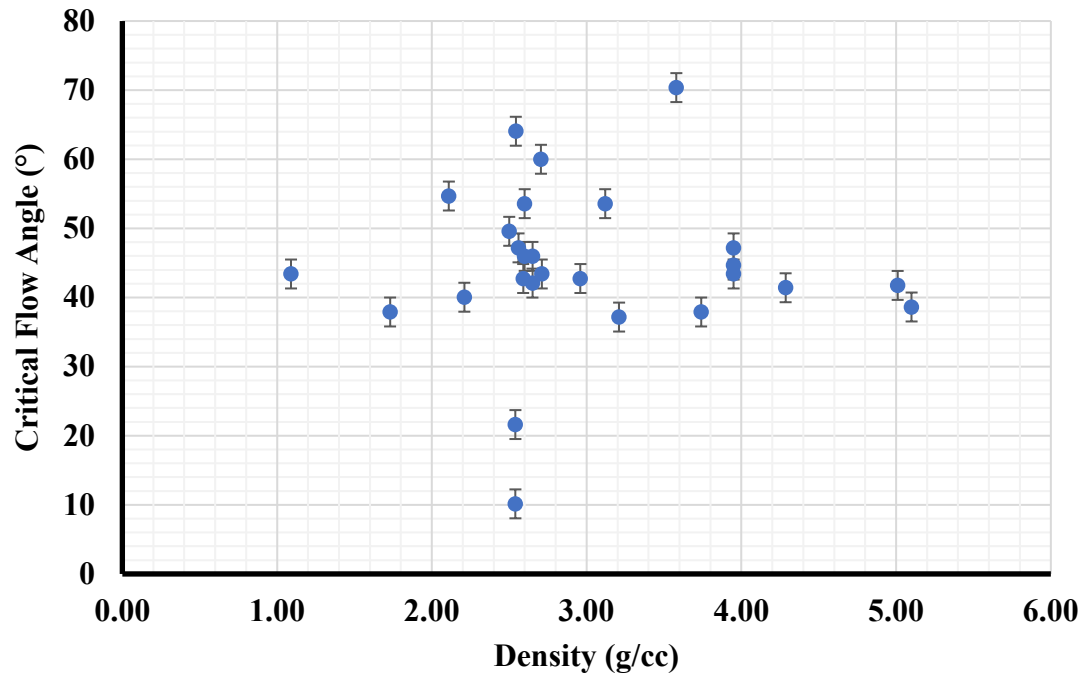


Figure 6. Plot of density of particles and their critical flow angles

Figure 6 illustrates that there is not a strong correlation between the density of a particle and the critical flow angle that that powder experiences. It can be concluded then that the hypothesis that density directly correlates to powder flow is incorrect. Figure 7 shows the relationship between first and critical flow angles.

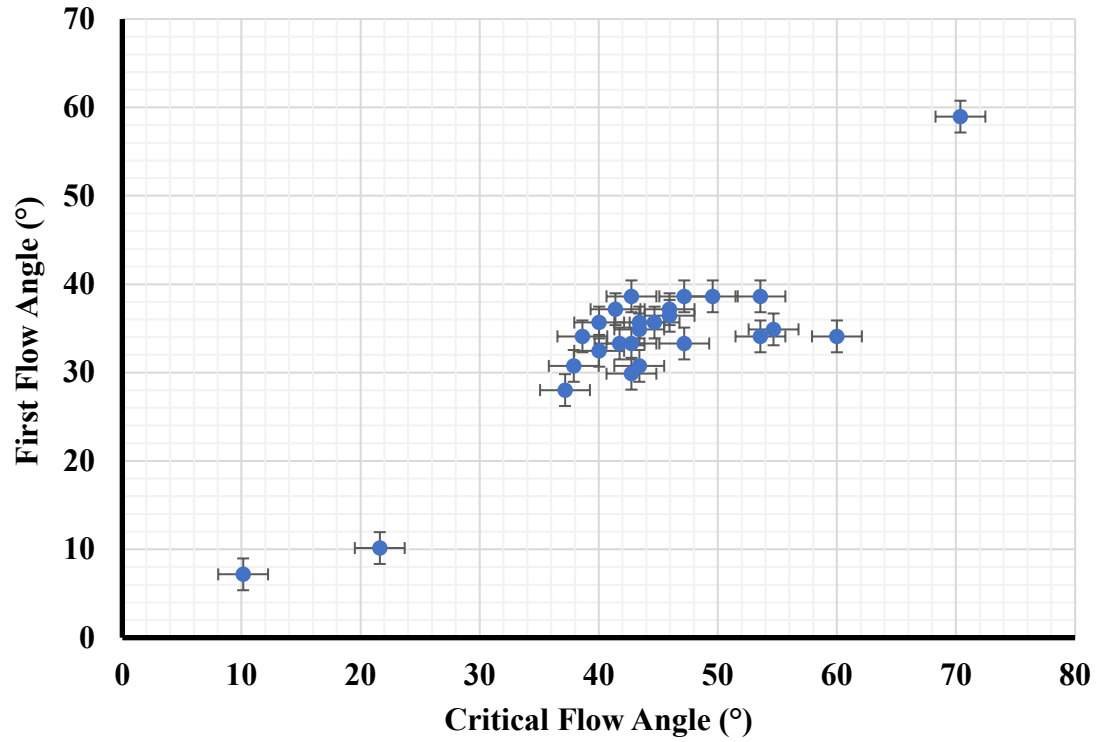


Figure 7. Plot of first flow and critical flow angles

There is a trend in this relationship which shows that if a powder has a high critical flow angle, then that powder will usually be observed to have a relatively high first flow angle. The next figure, Figure 8, shows the relationship between the ratio of critical flow angle and first flow angle ($\frac{\text{Critical Flow Angle}}{\text{First Flow Angle}}$), and the particle density.

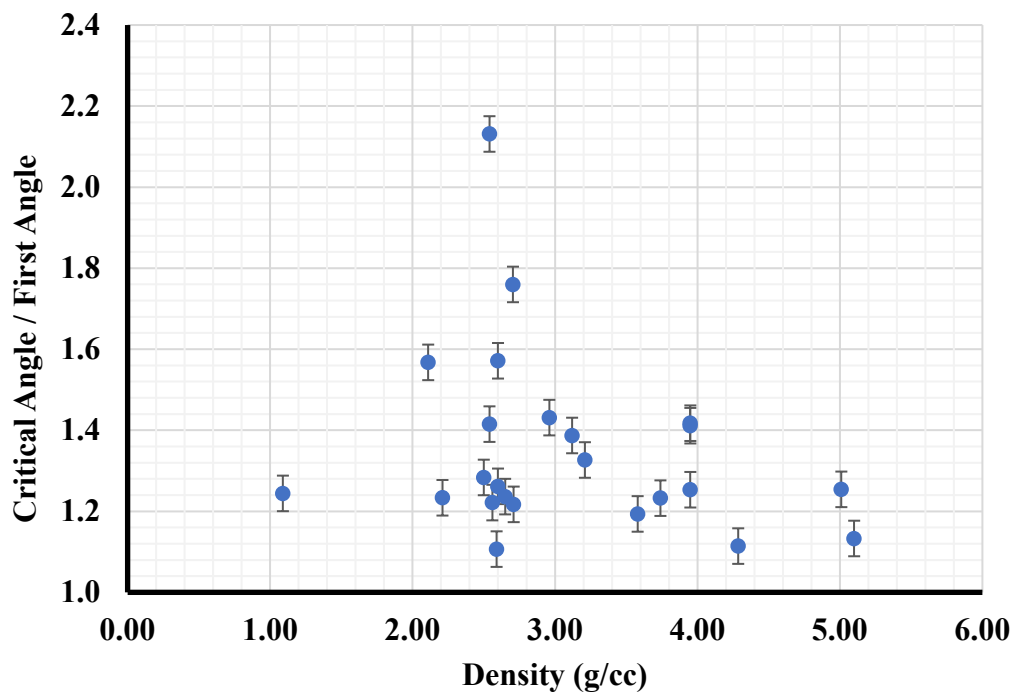


Figure 8. Plot of critical to first flow ratio and particle density

Figure 8 shows that even if a powder shows a large difference between critical flow and first flow, the density of the particle still does not have any correlation with the flowability of the powder. Figure 9 shows the relationship between particle mass and the calculated particle mass.

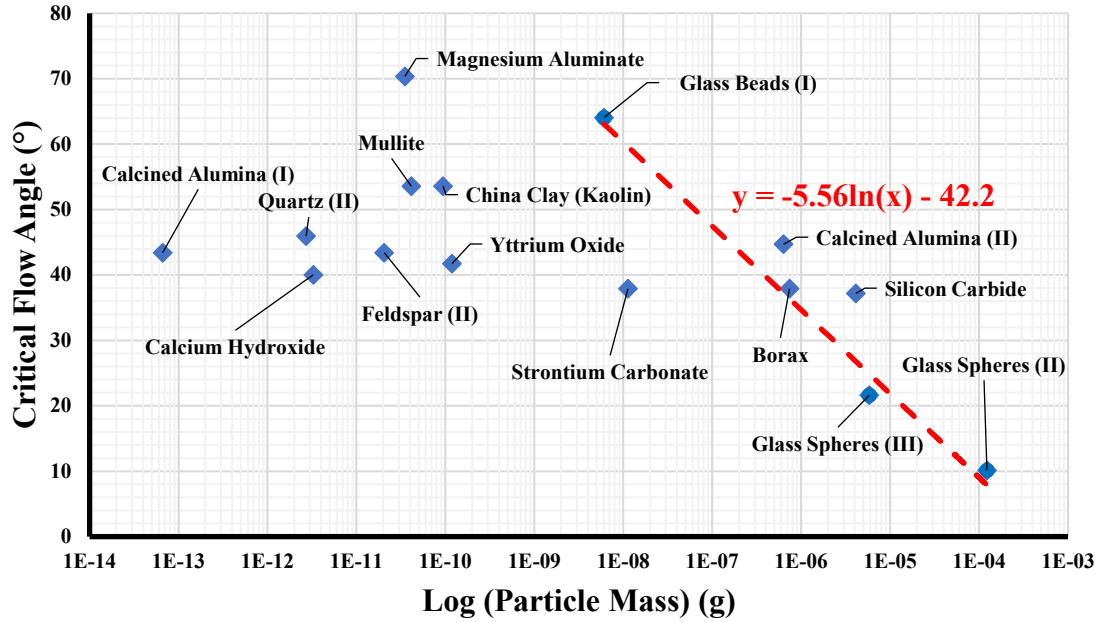


Figure 9. Plot of Critical Flow angle and log (Particle Mass).

The information in Figure 9 shows the calculated line for particle free flow, which is the red dotted line. It follows the equation

$$y = -5.56 \ln(\text{mass}_{\text{particle}}) - 42.2. \quad (7)$$

This line was chosen since it runs straight through the three glass sphere samples used in this experiment, which are shown imaged in Figures 11, 12, and 13. The glass spheres are considered perfect particles for flowability and the line is the separator between flowing and non-flowing powders. The flowing powders are to the right of the line and the non-flowing powders can be found to the left. Rather than coming up with a critical particle size necessary for particle free flow, an equation that changes with size and density is a better barrier and is more accurate as well. Figure 10 shows the

relationship between particle mass and angular velocity, as calculated from Equations 4 and 6.

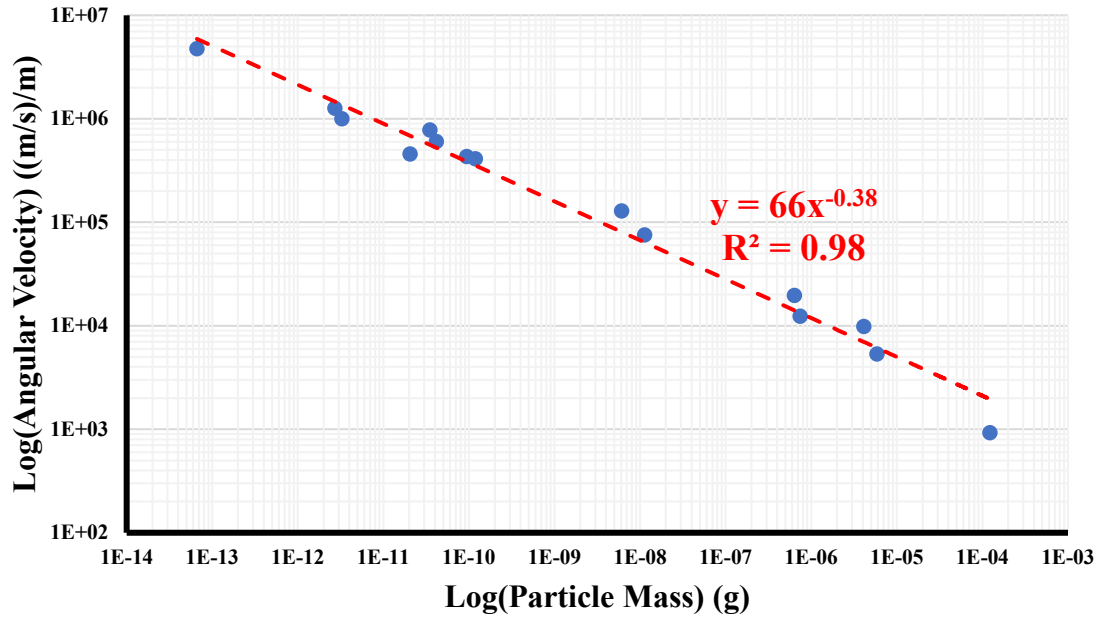


Figure 10. Plot of angular velocity versus particle mass.

Figure 10 is an important figure. It shows that with decreasing particle mass, the angular velocity increases. This is important since the less massive particles correlate with a higher angular velocity which means they must be flowing at higher angles when compared to the more massive particles. The correlation in data can be defined by Equation 8:

$$y = 66 * x^{-0.38} \quad (8)$$

4.3 Images of particles

Figures 11, 12, and 13 present the SEM images of the three glass standards used in this study. These are the only materials assumed to have free flow behavior. Therefore, they were used to try to determine a boundary for critical particle mass.

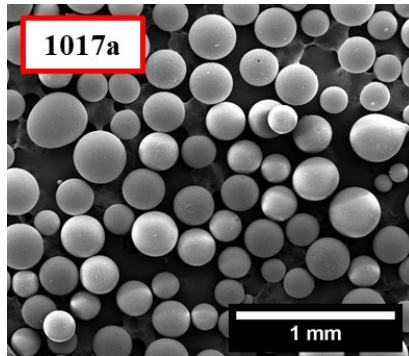


Figure 11. SEM images of glass sphere standard 1017a (Glass Spheres (III)).

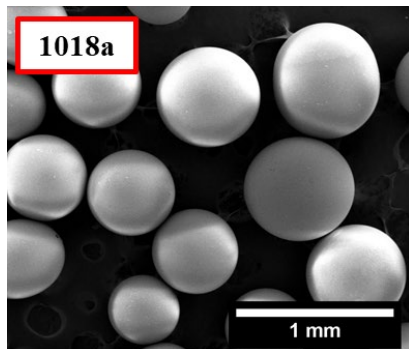


Figure 12. SEM images of glass sphere standard 1018a (Glass Spheres (II)).

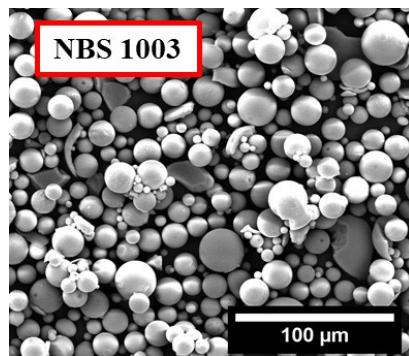


Figure 13. SEM images of glass sphere standard NBS 1003 (Glass Beads (I)).

Figures 14-19 shows a range of SEM images for critical flow samples. The borax, silicon carbide, and calcined alumina (II) or A-10 have large particles and are included in

the assumed free flow area in Figure 9. Grolleg or china clay and strontium carbonate have slightly smaller particles and sit in the middle of the graph. Calcined alumina (II) or A-16 is on the other side of the graph, with a small particle size under $1\text{ }\mu\text{m}$. The size effects demonstrated in Figure 9 is evident with A-10 and A-16, where they have drastically different sizes and therefore sit on opposite ends of the plot.

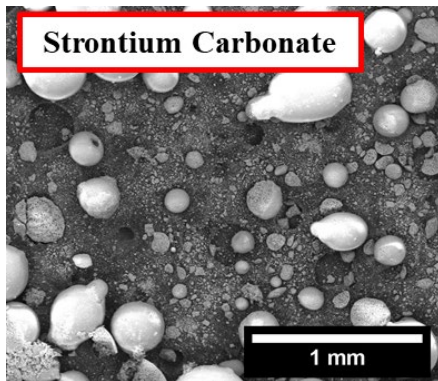


Figure 14. SEM image of critical flow for Strontium Carbonate.

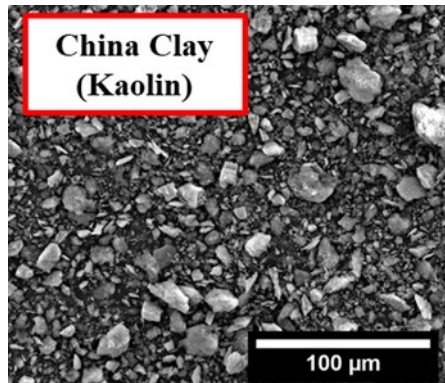


Figure 15. SEM image of critical flow for China clay (Kaolin).

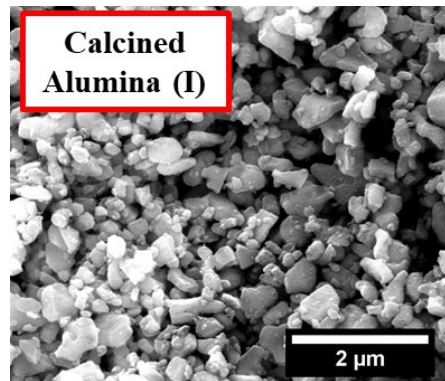


Figure 16. SEM image of critical flow for calcined alumina (I).

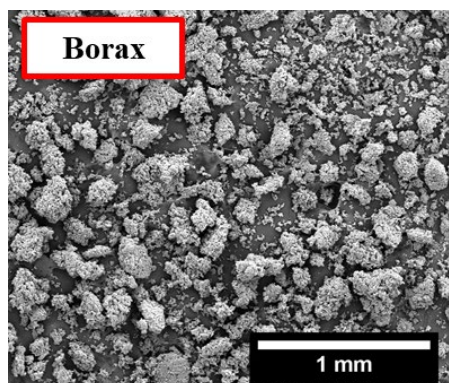


Figure 17. SEM image of critical flow for Borax.

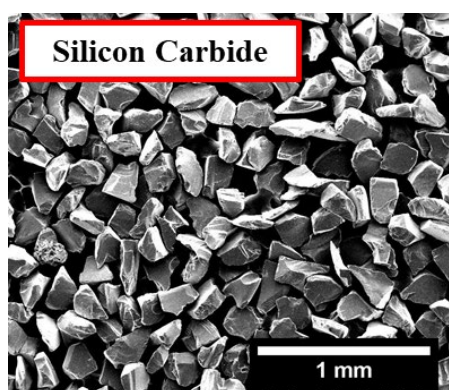


Figure 18. SEM image of critical flow for Silicon Carbide.

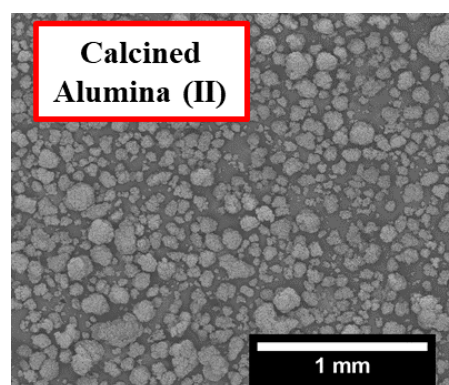


Figure 19. SEM image of critical flow for calcined alumina (II).

Figures 20, 21, 22 and 23 demonstrate the differences between critical and first flow samples of china clay and quartz (II), respectively. The first flow samples were thought to be mainly agglomerates and larger particles, which is supported by the visibly larger particles seen in Figures 20, 21, 22, and 23 for first flow. In contrast, critical flow is assumed to be true powder flow, where the material begins to flow as gravitational forces overcome the interparticle forces. Consequently, these particles are slightly smaller

and potentially more broadly distributed. Although literature indicates that agglomeration of particles is an important consideration, this study concludes that it is negligible and can be ignored.¹ The data in this study does not account for agglomeration. However, if agglomeration were to be accounted for, the resulting change in mass is inconsequential on a log scale.

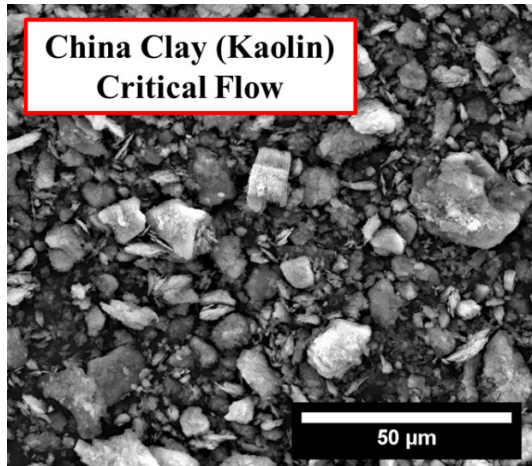


Figure 20. SEM images of china clay critical flow samples.

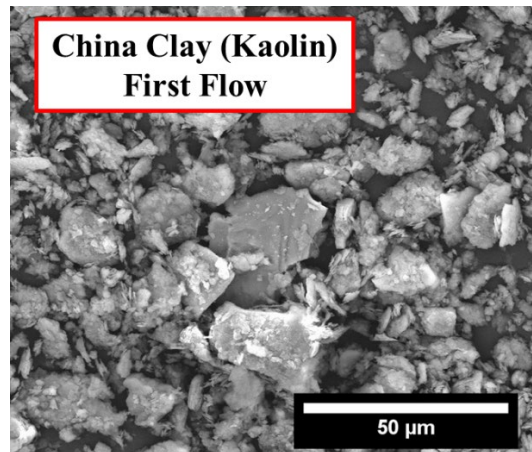


Figure 21. SEM images of china clay first flow samples.

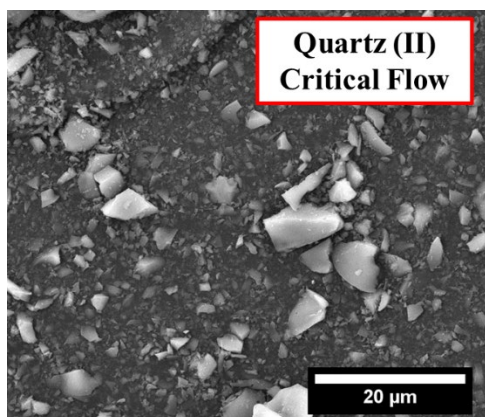


Figure 22. SEM images of quartz (II) critical flow samples.

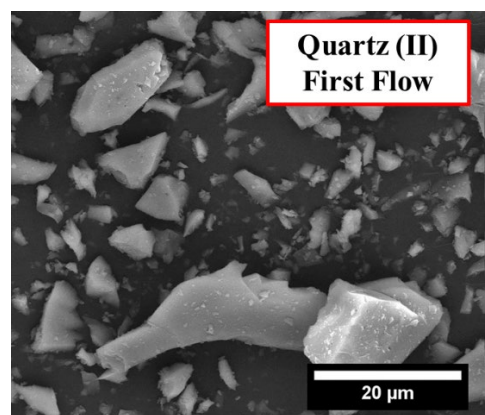


Figure 23. SEM images of quartz (II) first flow samples.

The data supports the conclusion that flow is independent of density.⁶ This is evident in Figure 9, where both calcined alumina samples reside on opposite sides of the plot, despite possessing the same density. This suggests that there is a size effect rather than a density effect. Changes to the density result in small changes on a log scale, thereby indicating that flow is independent of density. Literature supports these conclusions, particularly in relation to size segregation. A dominant factor in size segregation is the size difference of the particles, therefore size segregation can be reduced or prevented by decreasing the size of the particles.¹³ In Figure 9, the opposite appears to be true, an increase in particle size allows for better flow. It can also be concluded that the results are mass independent and are consistent with Galileo's results.

One of the many experiments Galileo is famous for is his experiment of falling bodies. Galileo dropped two spheres of differing masses from the Leaning Tower of Pisa in Italy and they hit the ground simultaneously. This directly contradicted the Aristotelian thought at the time that objects fell in speeds directly proportional to their weight.¹⁶

5. Conclusion

In this study, powders were analyzed to test the hypothesis that there is a correlation between particle size, density and flow behavior, and there is a critical particle mass necessary for free flow. The results of these experiments disagree with this hypothesis indicating that the hypothesis is incorrect. The literature concluded that density is not a variable and that conclusion is supported by these experiments in which angular velocity is solely a function of mass, not density. In addition, agglomeration increases the mass of the particle but does not appear to play an important role in the flow behavior. One reason for this may be that a change in density of 2x would not significantly shift the mass 0 values on the log-mass plot, therefore agglomeration can be ignored. There is not a critical particle mass necessary for powder free flow. It was found that angular velocity correlates with particle mass and can be defined with an exponential relationship. It can be said that the results of this experiment are consistent with the findings of Galileo Galilei, where between 1589 and 1592, he proved that different spheres with different masses fell off the Tower of Pisa and hit the ground simultaneously, in that our results are mass independent.

6. Future Work

Future work would include testing additional materials with the same density and various sizes. Some materials of interest would be alumina, quartz, and additional glass sphere standards. The goal of this future work is to better outline a minimum size for free flow and to further understand the relationship between flow behavior and size. Testing should also include scalped and un-scalped particle distributions. This comparison is relevant as most suppliers scalp a material to provide specific ranges to the consumer. This current study proves that size is a significant factor in flow, therefore it would be interesting to explore the flow behavior of a material that has been artificially manipulated.

7. References

1. Sinka IC, Schneider LCR, Cocks ACF. Measurement of the flow properties of powders with special reference to die fill. *Int J Pharm.* 2004;280(1–2):27–38. <https://doi.org/10.1016/j.ijpharm.2004.04.021>
2. Reed JS. Principles of Ceramic Processing. 2nd Editio. New York: John Wiley & Sons, Inc; 1995
3. Chirone R, Barletta D, Lettieri P, Poletto M. Bulk flow properties of sieved samples of a ceramic powder at ambient and high temperature. *Powder Technol.* 2016;288:379–387. <https://doi.org/10.1016/j.powtec.2015.11.040>
4. Van Burkalow A. Angle of repose and angle of sliding friction: An experimental study. *Bull Geol Soc Am.* 1945;56(6):669–707. [https://doi.org/10.1130/0016-7606\(1945\)56\[669:AORAAO\]2.0.CO;2](https://doi.org/10.1130/0016-7606(1945)56[669:AORAAO]2.0.CO;2)
5. Wong ACY. Use of angle of repose and bulk densities for powder characterization and the prediction of minimum fluidization and minimum bubbling velocities. *Chem Eng Sci.* 2002;57(14):2635–2640. [https://doi.org/10.1016/S0009-2509\(02\)00150-1](https://doi.org/10.1016/S0009-2509(02)00150-1)
6. Zhou YC, Xu BH, Yu AB, Zulli P. An experimental and numerical study of the angle of repose of coarse spheres. *Powder Technol.* 2002;125(1):45–54. [https://doi.org/10.1016/S0032-5910\(01\)00520-4](https://doi.org/10.1016/S0032-5910(01)00520-4)
7. Wouters IMF, Geldart D. Characterising semi-cohesive powders using angle of repose. *Part Part Syst Charact.* 1996;13(4):254–259. <https://doi.org/10.1002/ppsc.19960130408>
8. Geldart D, Abdullah EC, Hassanpour A, Nwoke LC, Wouters I. Characterization of powder flowability using measurement of angle of repose. *China Particuology.* 2006;4(3–4):104–107. [https://doi.org/10.1016/s1672-2515\(07\)60247-4](https://doi.org/10.1016/s1672-2515(07)60247-4)

9. Shah RB, Tawakkul MA, Khan MA. Comparative evaluation of flow for pharmaceutical powders and granules. *AAPS PharmSciTech*. 2008;9(1):250–258. <https://doi.org/10.1208/s12249-008-9046-8>
10. Wing ZN, Halloran JW. Dry Powder Deposition and Compaction for Functionally Graded Ceramics. *J Am Ceram Soc*. 2006;89(11):3406–3412. <https://doi.org/10.1111/j.1551-2916.2006.01272.x>
11. Sinka IC, Cocks ACF. Evaluating the flow behaviour of powders for die fill performance. *Powder Metall*. 2009;52(1):8–11. <https://doi.org/10.1179/174329009X441736>
12. Ashish J, Swaroop G, Balasubramanian K. Effect of Ammonium Perchlorate Particle Size on Flow, Ballistic, and Mechanical Properties of Composite Propellant. *Nanomater. Rocket Propuls. Syst*. Elsevier; 2018:299–362. <https://doi.org/10.1016/B978-0-12-813908-0.00008-3>
13. Liu G. Understanding and Minimizing Powder Segregation. *PowderbulkCom*. 2018;(May).
14. NIST. NIST - 301.1 - Particle Size (powder and solid forms). n.d.
15. Howles JA. Incorporation of Boron Compounds into a Whiteware Body. Alfred University; 1998
16. J.J. F. Galileo, His Life and Work. London: James Pott & Company; 1903